micro

MDPI

Communication

Stable $Cu_2P_3I_2$ and $Ag_2P_3I_2$ Single-Wire and Thin Film Devices for Humidity Sensing

Gregory R. Schwenk †, John T. Walters † and Hai-Feng Ji *

Department of Chemistry, Drexel University, Philadelphia, PA 19104, USA; grs72@drexel.edu (G.R.S.); jtw88@drexel.edu (J.T.W.)

* Correspondence: hj56@drexel.edu; Tel.: +1-215-895-2562; Fax: +1-215-895-1265

† These authors contributed equally to this work.

Abstract: $Cu_2P_3I_2$ wires were synthesized and converted to $Ag_2P_3I_2$ via post-synthetic modification. Single-wire and thin film devices were constructed from each material and evaluated as rapidly reversible humidity sensing semiconductors. All devices exhibited a dramatic increase in current when exposed to a ~30.85% RH (~9745.3 ppm by moisture volume) atmosphere compared to that of dry N_2. $Cu_2P_3I_2$ devices exhibited greater sensitivity compared to their respective $Ag_2P_3I_2$ analogs with the highest being the thin film at $2.43 \times 10^{-8} \frac{A}{\% RH}$. While all devices exhibited rapid (<5 s) reversibility, the thin film devices exhibited greater sensitivity compared to their single-wire forms.

Keywords: moisture sensor; phosphorus nanomaterials; metal phosphorus halide

Citation: Schwenk, G.R.; Walters, J.T.; Ji, H.-F. Stable $Cu_2P_3I_2$ and $Ag_2P_3I_2$ Single-Wire and Thin Film Devices for Humidity Sensing. *Micro* **2022**, 2, 183–190. https://doi.org/10.3390/micro2010012

Academic Editor: Hiroshi Furuta

Received: 11 January 2022
Accepted: 28 February 2022
Published: 3 March 2022

1. Introduction

Since the discovery of phosphorene, phosphorus-based materials have received a dramatic increase in research interest. These materials are composed of various allotropic forms of phosphorus, such as type I (amorphous) red [1], type IV (fibrous) red [2], type V (violet/Hittorf's) red [3], black phosphorus [4], etc. Owing to their unique electronic properties, these forms of phosphorus have been employed as various electronic [5] and optoelectronic [6] devices. They have also been used for other applications, such as photocatalysts [7].

One application of such an electronic device is a molecular sensor. The electronic response of such devices may be monitored in the presence of various atmospheres, such as humidity, resulting in a definitive change. However, all allotropic forms of phosphorus often present the significant drawback of air-instability. Such instability, particularly in the case of black phosphorus, is believed to be the result of slow oxidation in O_2-rich and humid atmospheric conditions [8]. To construct any useful electronic device suited for molecular sensing, efforts must be made to stabilize the material without compromising its electronic properties. Recently, while developing black phosphorus humidity sensors, several attempts have been made to stabilize air-sensitive phosphorus-containing devices, however these methods often employ surface passivation techniques [9,10]. Since molecular sensing often depends heavily on the interaction of the pristine surface of the material with the analyte, such passivation techniques obviously mitigate device efficacy. To the best of our knowledge, no research efforts have been established to produce a reversible air-stable humidity sensor utilizing a pure phosphorus-based material. Herein, we report our preliminary study on two phosphorus-based materials that exhibit such enhanced stability and variable conductivity in the presence of atmospheres of varying humidity: $Cu_2P_3I_2$ and $Ag_2P_3I_2$.

$Cu_2P_3I_2$ presents an interesting material that has been identified as an effective air-stable semiconductor capable of high ionic mobility [11]. Crystallizing in a needle-like fashion, the Cu atoms loosely occupy positions around phosphorus tubes composed of a P_8-P_4 repetition, exhibiting a motif reminiscent of Hittorf's (Violet) Phosphorus [12]. These Cu

atoms are externally surrounded by localized I atoms, thereby extending in one-dimension to produce a wire. As suggested by the crystallographic data and confirmed by facile aqueous ion-exchange reactions to form $Ag_2P_3I_2$, these wires exhibit ionic mobility in the layer between phosphorus and iodine [13]. As a result, these materials present themselves as promising and robust single-wire electronic devices.

Although lacking the central phosphorus tube, the parent material of $Cu_2P_3I_2$, CuI, is also a well-known ionic conductor [14]. Existing as a powder, thin films of CuI have been reported to exhibit semiconducting character that changes reversibly as a function of relative humidity exposure. Particularly, these materials have exhibited a maximum conductivity enhancement near 30% RH [15]; this property may be possible to impart on the $Cu_2P_3I_2$ materials. Conversely, the parent material of the $Ag_2P_3I_2$ analog, AgI, is also a well-known ionic conductor [16], but, to our knowledge, has not been documented as a humidity sensor. However, AgI has been reported as an effective ice-nucleating material [17]. Such favorable interactions with water suggest this material may also exhibit detectable changes in conductivity upon humidity exposure, especially at low moisture level. The scope of this study entails the synthesis of both $Cu_2P_3I_2$ and $Ag_2P_3I_2$ for the purpose of producing both single-wire and thin film fully reversible humidity-sensing electronic devices.

2. Materials and Methods

2.1. Synthesis of $Cu_2P_3I_2$

Targeting a 100 mg product yield, stoichiometric amounts of the constituent atoms were combined in a way similar to a previous report from this lab [11]. Following the same procedure, the resulting wires exhibited the same morphology and approximate size. Briefly, 19.6 mg of Type I (amorphous red) phosphorus and 80.2 mg of CuI were added to a borosilicate tube, which was then backfilled with argon and evacuated. The tube was then sealed as an ampoule under vacuum. Multiple trials were run at once. Spaced evenly in the in the center, the ampoules were added to a muffle furnace. The temperature of the furnace was raised to 373 K then heated to 723 K at a rate of 5 K/min. The furnace was then heated at a rate of 1 K/min until 823 K, which was subsequently heated at a rate of 0.5 K/min until 853 K. The furnace was further heated until 859 K at a rate of 0.13 K/min then to 863 K at 0.07 K/min where it was held for 48 h. The furnace was cooled to 859 K at a rate of 0.07 K/min then to 823 K at a rate of 0.13 K/min. The furnace was then cooled to 723 K at a rate of 0.33 K/min where it was held for 18 h. The furnace was then cooled at a rate of 5 K/min until reaching 473 Kwhere the furnace was turned off and allowed to equilibrate naturally to room temperature. $Cu_2P_3I_2$ formed wires of 3–5 mm in urchin-like patches throughout the ampoule.

2.2. Synthesis of $Ag_2P_3I_2$

As described by Möller and Jeitschko [13], $Cu_2P_3I_2$ wires were added to a 10% w/w aqueous $AgNO_3$ solution in the presence of excess KCN to facilitate the following ion-exchange reaction.

$$Cu_2P_3I_2 + 2[Ag(CN)_2]^- + 4CN^- \rightarrow Ag_2P_3I_2 + 2[Cu(CN)_4]^{3-}$$

The reaction mixture was allowed to sit for a few hours. The mixture was then centrifuged, and the supernatant was siphoned off. The remaining $Ag_2P_3I_2$ was washed by suspending the solid in methanol. The resulting suspension was centrifuged, and the supernatant was siphoned off.

2.3. Preparation of Thin Films

Approximately 30 mg of phosphorus metal halide was added to a mortar, and N-Methyl-2-pyrrolidone (NMP) was added to facilitate liquid-assisted grinding. The phosphorus metal halide was grinded until fine and was then added to a 50 mL centrifuge tube. NMP was added until the mixture volume reached 35 mL. The mixture was then sonicated at ultrahigh frequencies via a sonifier homogenizer for 3 h. The resulting sonicated

suspension was then transferred to smaller vessels and centrifuged at 13,000× *g* rpm for 15 min. The supernatant was removed, and the solid was collected with methanol. The new suspension was then briefly sonicated and dropcasted onto a Si/SiO_2 (n-doped) wafer with two gold plates separated by a 10-micrometer channel (Figure 1) such that any source voltage would be required to flow through the material to go to ground.

(**a**) (**b**)

Figure 1. Fully rendered image of pristine (**a**) and film-coated (**b**) Si/SiO_2 wafer containing 2 gold electrodes separated by a 10-µm channel (rendered in Fusion 360).

2.4. Electrical Characterization

IV measurements were conducted using a Keithley 2636A Dual-channel System SourceMeter Instrument. Single wire devices were constructed by connecting two gold electrodes on a Si/SiO_2 substrate with a single wire (~3–5 mm in length) attached with graphene-based conductive glue. Thin film devices were generated in a similar fashion, but did not require conductive paste to the wafer. Copper wires were attached, also with the graphene-based conductive glue, to each of the gold electrodes which were connected to the single wire and thin film devices, allowing connection to the instrument for source and drain voltages. Current was measured over a time varying applied electric potential.

2.5. Humidity Controlled Atmospheres

Fixed-humidity atmospheres were achieved through saturated binary salt solutions and were prepared in scintillating vials with tailored humidity values according to Greenspan's least squares equations [18]. Briefly, the caps to 20 mL scintillating vials were removed, and the cardboard lining was removed. Any remaining glue was scraped off, and the cap was washed with acetone. Two holes were made in the side of the cap directly opposite of each other. The circumference and top of the cap were wrapped in parafilm. The devices were taped to the inside of the cap, and the copper wires were poked through the parafilm and glued to the gold electrodes on the wafer which was now fixed to the inside of the cap (Figure 2). The saturated salt solution of KF inside the vial achieved a relative humidity of ~30.85% (~9745.3 ppm by moisture volume) [19] in the remaining headspace where the device was exposed. This fixed humidity is the result of the colligative vapor pressure depression resulting from a saturated binary salt solution. The value here is defined, at a given temperature, by the vapor pressure generated by the saturated solution divided by the vapor pressure of pure water times 100. The ambient temperature of the lab fluctuated between 25.0 and 25.6 °C; the difference in the relative humidity at this temperature range is insignificant. A nitrogen atmosphere was created to approximate 0% RH by passing 99.999% pure N_2 through a drying column and into a scintillating vial where device exposure would occur. The devices were placed in a vacuum oven (40 °C) for 20 min then sealed on top of the scintillating vial containing the saturated salt solution with a headspace reflecting the desired humidity. Electrical characterization was performed while the cap was sealed on the vial. Trials were run immediately (~2 min after sealing the vial) then at 4, 6, 8, and 10 min after exposure to ensure consistency. The cap would then be removed, and another measurement was immediately taken in ambient conditions. The measurement in ambient conditions, as opposed to dry N_2, was taken directly after KF exposure to best assess the rapid response to atmospheric changes with minimal time between measurements.

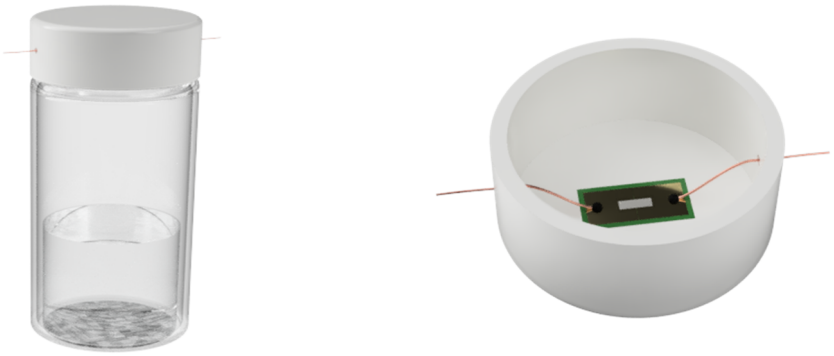

(**a**) (**b**)

Figure 2. (**a**) Fully rendered image of the chamber in which the material was exposed to the fixed humidity, (**b**) and the inside of the cap where the device was taped (images rendered in Fusion 360).

3. Results and Discussion

When exposed to relative humidity-controlled atmospheres, the conductivity of the materials increases by orders of magnitude (Figure 3). Each device (200 mV applied potential) displays a dramatic increase in the magnitude of current when exposed to ~30.85% RH (~9745.3 ppm by moisture volume) that was prepared from the vapor of a saturated solution of KF [18], when compared to that of the dry N_2 standard. In all cases, the thin films display a greater change in current in response to RH, suggesting these devices to be more sensitive than their single-wire analogs (Table 1). The potential influences the thin film process may have on electronic properties (i.e., grinding, sonication, solvent suspension, etc.) has not been assessed in this work and will be investigated in a future study.

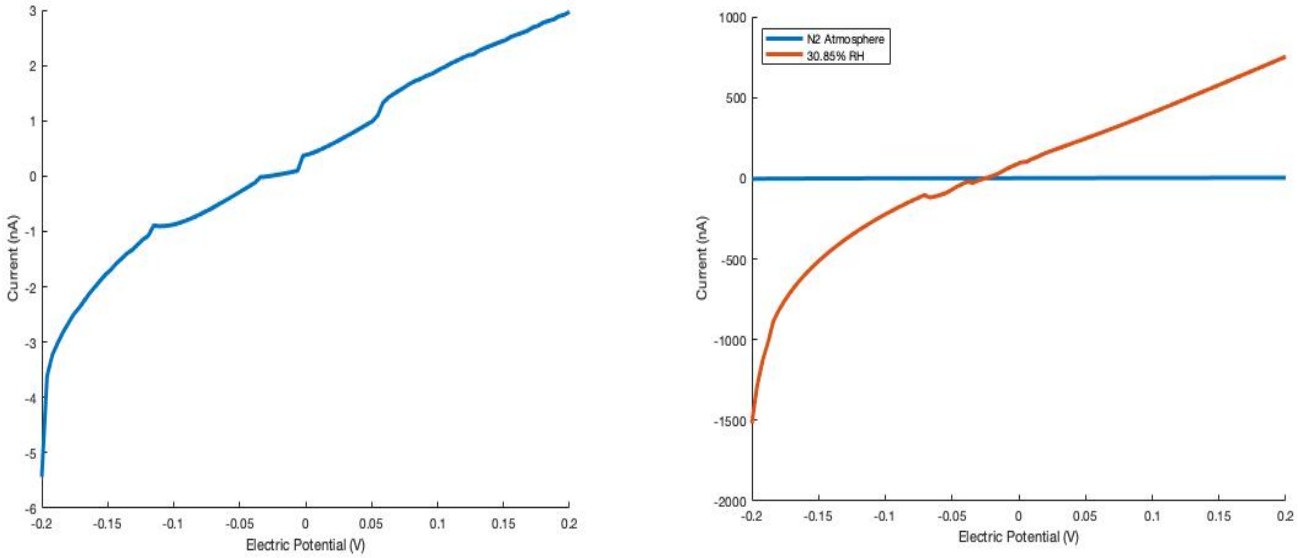

(**a**) (**b**)

Figure 3. *Cont.*

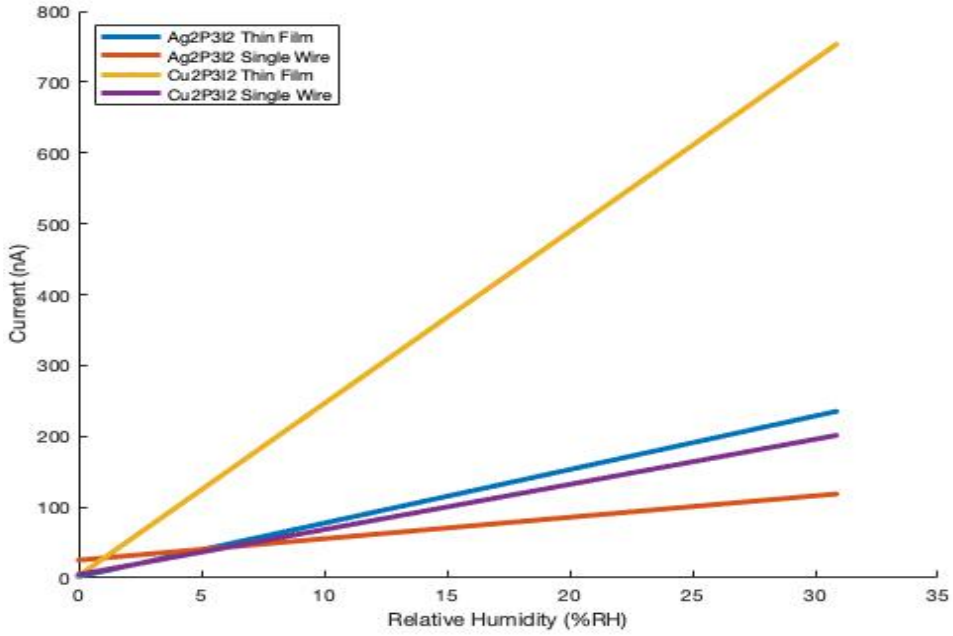

(**c**)

Figure 3. $Cu_2P_3I_2$ thin film device displaying dramatically increased current when exposed to the atmosphere generated from the vapor of a saturated solution of KF (~9745.3 ppm by moisture volume), compared to dry N_2 (**a**,**b**). Influence of humidity on current of single-wire and thin film devices of $Cu_2P_3I_2$ and $Ag_2P_3I_2$ (**c**).

Table 1. Sensitivity of each device rationalized as the change in current over a given range of atmospheric conditions.

Material	Type of Device	Sensitivity in the 0–~30.85% RH Range ($\frac{A}{\%\,RH}$)
$Cu_2P_3I_2$	Thin film	2.43×10^{-8}
$Cu_2P_3I_2$	Single wire	6.37×10^{-9}
$Ag_2P_3I_2$	Thin film	7.59×10^{-9}
$Ag_2P_3I_2$	Single wire	3.04×10^{-9}

Furthermore, the effect of humidity on conductivity is quickly reversible. To assess the reversibility, each device was exposed to a fixed-humidity vapor atmosphere generated by a saturated solution of NaCl. The devices were held under the fixed-humidity atmosphere for 10 min before the caps were removed and the IV curve was generated again. By the time the cap was taken off and room condition measurements were being acquired, the IV curve was already dramatically different. Thus, $Cu_2P_3I_2$ thin film devices exhibit rapid (<5 s) reversibility when returning to ambient conditions (Figure 4). The $Cu_2P_3I_2$ single wire devices, $Ag_2P_3I_2$ single wire devices, and $Ag_2P_3I_2$ thin film devices all displayed similar responses.

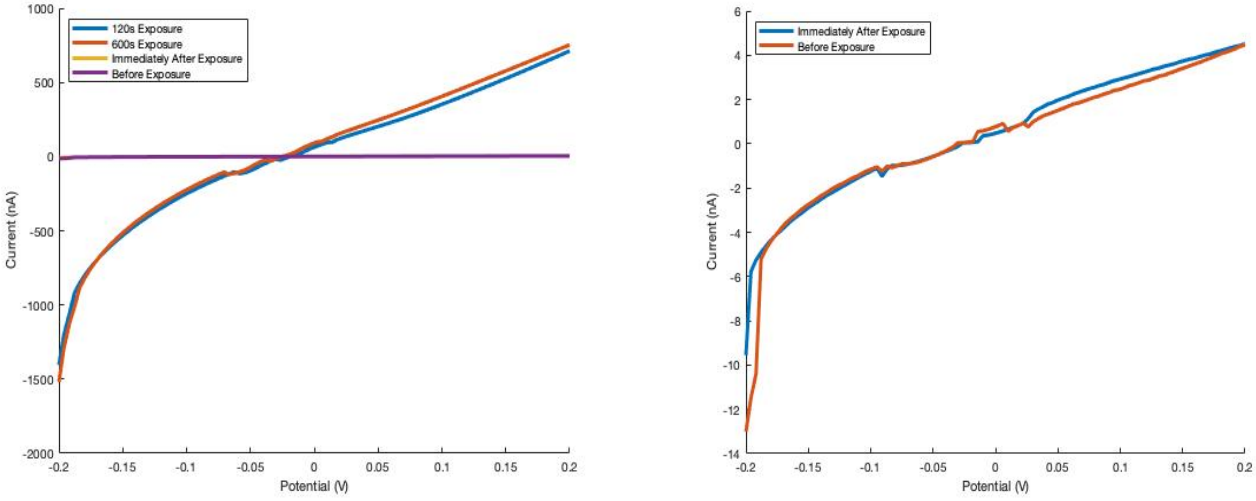

(**a**) (**b**)

Figure 4. Reversibility of humidity influence (fixed-humidity atmosphere data acquired directly before ambient atmosphere) for thin films of $Cu_2P_3I_2$. (**a**) The drastic changes in current induced by an atmosphere containing 30.85% RH were found to be quickly reversible (<5 s) despite a 10-min exposure. (**b**) The image on the right omits the IV curves from the 30.85% RH atmosphere for clarity.

As expected, thin film and single-wire devices of the two materials, $Cu_2P_3I_2$ and $Ag_2P_3I_2$ were tested and proven to maintain their conductivity reliably in air. The conductivity remained largely the same in all cases after at least 10 days for $Cu_2P_3I_2$ (Figure 5), which is similar to that of $Ag_2P_3I_2$. As mentioned in the introduction section, one of the greatest drawbacks of pure phosphorus-based materials applied as sensors is their low stability in air. Over a time of 10 days, other phosphorus-based materials suffer oxidation, resulting in a significant decrease in conductivity [1]. Owing to its isolation and strong atomic interactions, oxidation is prohibited in the $Cu_2P_3I_2$ and $Ag_2P_3I_2$ materials, since P interacts strongly with metal iodides.

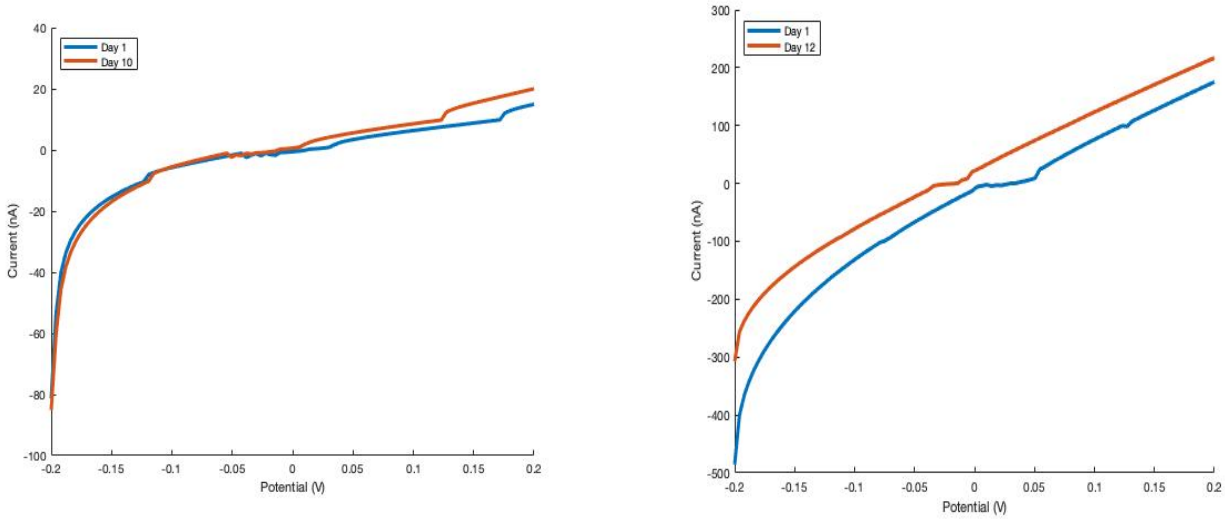

(**a**) (**b**)

Figure 5. $Cu_2P_3I_2$ thin film (**a**) and single-wire (**b**) devices exhibit comparable current when tested several days apart after exposure to a constant atmosphere (~75% RH).

4. Conclusions

Both thin films and single-wire devices of $Cu_2P_3I_2$ and $Ag_2P_3I_2$ were constructed and evaluated as stable humidity-sensing devices. Each device was exposed to atmospheres containing dry N_2 and ~30.85% RH (~9745.3 ppm by moisture volume), and the resulting IV curve was observed. The conductivities of the devices remain roughly the same after 10 days. Across both materials and device compositions (i.e., single-wire, thin film) the conductivity increases drastically when exposed to ~30.85% RH (~9745.3 ppm by moisture volume) atmosphere, bearing similarity to CuI thin film devices. In all cases semiconducting nature was maintained and any changes were fully reversible within seconds upon re-exposure to original conditions. The $Cu_2P_3I_2$ thin films exhibited a much larger shift (~10^3) in current from dry atmosphere to ~30.85% RH (~9745.3 ppm by moisture volume) when compared to the $Ag_2P_3I_2$ analog, suggesting greater sensitivity. In both materials, the thin films present greater sensitivity over their single-wire device analogs. This preliminary study shows the potential sensing capability of $Cu_2P_3I_2$ and $Ag_2P_3I_2$ single-wire and thin film devices with high stability.

Author Contributions: G.R.S. and J.T.W. performed the experiments and analyzed the data. H.-F.J. provided the laboratory space and materials with which the experiments were conducted. All the authors have contributed to the design of the experiments, writing, and editing of the paper. All authors have read and agreed to the published version of the manuscript.

Funding: This research received no external funding.

Institutional Review Board Statement: Not applicable.

Informed Consent Statement: Not applicable.

Conflicts of Interest: The authors declare no conflict of interest.

References

1. Amaral, P.E.M.; Nieman, G.P.; Schwenk, G.R.; Jing, H.; Zhang, R.; Cerkez, E.B.; Strongin, D.; Ji, H. High Electron Mobility of Amorphous Red Phosphorus Thin Films. *Angew. Chem. Int. Ed.* **2019**, *58*, 6766–6771. [CrossRef] [PubMed]
2. Zhang, G.; Liu, D.; Tian, N.; Liu, B.; Li, S.; You, C.; Qu, X.; Ma, H.; Fan, C.; Zhang, Y. Liquid Exfibration and Optoelectronic Devices of Fibrous Phosphorus. *Inorg. Chem.* **2020**, *59*, 976–979. [CrossRef] [PubMed]
3. Schusteritsch, G.; Uhrin, M.; Pickard, C.J. Single-Layered Hittorf's Phosphorus: A Wide-Bandgap High Mobility 2D Material. *Nano Lett.* **2016**, *16*, 2975–2980. [CrossRef] [PubMed]
4. Wu, Z.; Lyu, Y.; Zhang, Y.; Ding, R.; Zheng, B.; Yang, Z.; Lau, S.P.; Chen, X.H.; Hao, J. Large-Scale Growth of Few-Layer Two-Dimensional Black Phosphorus. *Nat. Mater.* **2021**, *20*, 1203–1209. [CrossRef] [PubMed]
5. Islam, A.; Feng, P.X.-L. Electronic Applications of Black Phosphorus Thin Films. In *Fundamentals and Applications of Phosphorus Nanomaterials*; Ji, H.-F., Ed.; ACS Symposium Series; American Chemical Society: Washington, DC, USA, 2019; Volume 1333, pp. 179–194. [CrossRef]
6. Dong, B.; Huang, L.; Lee, C.; Ang, K.-W. Black Phosphorus Based Photodetectors. In *Fundamentals and Applications of Phosphorus Nanomaterials*; Ji, H.-F., Ed.; ACS Symposium Series; American Chemical Society: Washington, DC, USA, 2019; Volume 1333, pp. 135–153. [CrossRef]
7. Liu, Y.; Li, J.; Hu, Z.; Yu, J.C. Photocatalytic Property of Phosphorus. In *Fundamentals and Applications of Phosphorus Nanomaterials*; Ji, H.-F., Ed.; ACS Symposium Series; American Chemical Society: Washington, DC, USA, 2019; Volume 1333, pp. 155–177. [CrossRef]
8. Marmolejo-Tejada, J.M.; Jaramillo-Botero, A. Effect of Surface Oxidation on the Electronic Transport Properties of Phosphorene Gas Sensors: A Computational Study. *RSC Adv.* **2020**, *10*, 6893–6899. [CrossRef]
9. Wood, J.D.; Wells, S.A.; Jariwala, D.; Chen, K.-S.; Cho, E.; Sangwan, V.K.; Liu, X.; Lauhon, L.J.; Marks, T.J.; Hersam, M.C. Effective Passivation of Exfoliated Black Phosphorus Transistors against Ambient Degradation. *Nano Lett.* **2014**, *14*, 6964–6970. [CrossRef] [PubMed]
10. Miao, J.; Cai, L.; Zhang, S.; Nah, J.; Yeom, J.; Wang, C. Air-Stable Humidity Sensor Using Few-Layer Black Phosphorus. *ACS Appl. Mater. Interfaces* **2017**, *9*, 10019–10026. [CrossRef] [PubMed]
11. Amaral, P.E.M.; Ji, H.-F. Stable Copper Phosphorus Iodide ($Cu_2P_3I_2$) Nano/Microwire Photodetectors. *ChemNanoMat* **2018**, *4*, 1083–1087. [CrossRef]
12. Zhang, L.; Huang, H.; Zhang, B.; Gu, M.; Zhao, D.; Zhao, X.; Li, L.; Zhou, J.; Wu, K.; Cheng, Y.; et al. Structure and Properties of Violet Phosphorus and Its Phosphorene Exfoliation. *Angew. Chem. Int. Ed.* **2020**, *59*, 1074–1080. [CrossRef]

13. Möller, M.H.; Jeitschko, W. Preparation, Properties, and Crystal Structure of the Solid Electrolytes Cu2P3I2 and Ag2P3I2. *J. Solid State Chem.* **1986**, *65*, 178–189. [CrossRef]
14. Yashima, M.; Xu, Q.; Yoshiasa, A.; Wada, S. Crystal Structure, Electron Density and Diffusion Path of the Fast-Ion Conductor Copper Iodide CuI. *J. Mater. Chem.* **2006**, *16*, 4393. [CrossRef]
15. Crovetto, A.; Hempel, H.; Rusu, M.; Choubrac, L.; Kojda, D.; Habicht, K.; Unold, T. Water Adsorption Enhances Electrical Conductivity in Transparent P-Type CuI. *ACS Appl. Mater. Interfaces* **2020**, *12*, 48741–48747. [CrossRef] [PubMed]
16. Yamamoto, T.; Maesato, M.; Hirao, N.; Kawaguchi, S.I.; Kawaguchi, S.; Ohishi, Y.; Kubota, Y.; Kobayashi, H.; Kitagawa, H. The Room-Temperature Superionic Conductivity of Silver Iodide Nanoparticles under Pressure. *J. Am. Chem. Soc.* **2017**, *139*, 1392–1395. [CrossRef]
17. Zielke, S.A.; Bertram, A.K.; Patey, G.N. A Molecular Mechanism of Ice Nucleation on Model AgI Surfaces. *J. Phys. Chem. B* **2015**, *119*, 9049–9055. [CrossRef]
18. Greenspan, L. Humidity Fixed Points of Binary Saturated Aqueous Solutions. *J. Res. Natl. Bur. Stand. Sect. A Phys. Chem.* **1977**, *81A*, 89. [CrossRef]
19. PST | Michell Humidity Calculator. Available online: https://www.processsensing.com/en-us/humidity-calculator/ (accessed on 17 February 2022).